



Identification of potential diagnostic biomarkers and immune infiltration features in diabetic foot ulcer by bioinformatics analysis and validation

Xiaohua Li^{1,2}, Biwu Chen³, Yuanyuan Xu⁴, Anbang Zhou⁴, Biaoliang Wu^{1,5*}

¹Medical School, Jinan University, Guangzhou 510632, Guangdong, China

²Department of Health Management Center, Affiliated Hospital of Youjiang Medical University for Nationalities, Baise 533000, Guangxi, China

³Department of Ultrasonography, Affiliated Hospital of Youjiang Medical University for Nationalities, Baise 533000, Guangxi, China

⁴Youjiang Medical University for Nationalities, Baise 533000, Guangxi, China

⁵Department of Endocrinology, Affiliated Hospital of Youjiang Medical University for Nationalities, Baise 533000, Guangxi, China

ARTICLE INFO

Original paper

Article history:

Received: June 17, 2023

Accepted: September 15, 2023

Published: November 15, 2023

Keywords:

Diabetic foot ulcer, circRNA, diagnose biomarker, immune cell infiltration, bioinformatics analysis

ABSTRACT

Diabetic foot ulcer (DFU) is the most serious and costly chronic complication that may lead to disability and even death in patients suffering from diabetes mellitus (DM). However, the clinical diagnosis and prognosis of DFU is inadequate. There is still a lack of effective biomarkers for its early diagnosis. We obtained the circRNA expression dataset GSE114248 and mRNA expression dataset GSE80178 from the GEO. R software was used to identify the differentially expressed circRNAs (DECs). The mRNAs associated with DFU were identified by a random forest algorithm and intersected with mRNAs predicted by circRNAs. Then, the circRNA-miRNA-mRNA network was established and the hub genes were screened using GO semantic similarity and were validated by the GSE199939 dataset. Meanwhile, the expression level of the biomarkers was verified by RT-PCR assays and immunohistochemistry. Finally, GSEA was conducted to determine differential immune cell infiltration and the immunological cells' relationships with hub genes. We identified three hub genes including *KIAA1109*, *ENPP5*, and *NRP1* that might play an important role in DFU. ROC curve results also showed a good performance of these three genes in the validation dataset. Furthermore, RT-PCR assays and immunohistochemistry confirmed the results above. Immune infiltration analysis indicated that DFU had a significant increase in Neutrophils. Moreover, three hub genes were closely correlated with a variety of inflammatory cells. *KIAA1109*, *ENPP5*, and *NRP1* are key hub genes of DFU. They might play an important role in the development of DFU and could be potential biomarkers in DFU.

Doi: <http://dx.doi.org/10.14715/cmb/2023.69.11.27>

Copyright: © 2023 by the C.M.B. Association. All rights reserved.

Introduction

DFU is one of the most common complications affecting the lower extremities in DM patients (1). According to the 2015 prevalence data of the International Diabetes Federation, it was estimated that 9.1 million to 26.1 million diabetic patients worldwide develop foot ulcers each year. Since DFU is associated with long-term complications of microvascular and macrovascular, it is necessary to detect the complications early. If the risk stratification of DFU can be obtained earlier in diabetic patients, the hospitalization, disability and mortality rate will be reduced (2). Therefore, exploring the effective diagnostic biomarkers of DFU is the focus of current research and is the key to the early diagnosis and treatment of DFU.

CircRNAs are an emerging class of noncoding RNA molecules that are widely expressed in mammalian tissues and have abundant binding sites for microRNAs (miRNAs) which participate in nearly all biological processes such as proliferation, differentiation, apoptosis and development, but also act as an important role in the pathogenesis of many diseases (3,4). Accumulating pieces of evidence indicate that circRNA acts as a miRNA sponge in competitive endogenous RNA (ceRNA) networks and plays

crucial roles in a variety of diseases (5-7). These findings provided clues to the molecular mechanism of DFU at the level of circRNA and mRNA. We can predict the progression of DFU from molecules related to the pathogenesis of DFU.

As bioinformatic technology rapidly advances, numerous data profiles from the GEO database have been re-analyzed by researchers. Integrated bioinformatics analyses of expression profiling by high throughput sequencing data derived from different investigations of DFU could help identify the novel diagnostic markers and further demonstrate their related functions and potential therapeutic targets in DFU.

In this study, the circRNA expression dataset and mRNA expression dataset which contain DFU and normal control samples were downloaded from the GEO. R software and the LIMMA package were used to identify the DECs. The random forest algorithm was used to identify the characteristic mRNA of DFU, which was intersected with the mRNA predicted by DECs. Then the circRNA-miRNA-mRNA network was established and the hub genes were screened using protein-protein interaction (PPI) analysis and GO semantic similarity. The GSE199939 dataset was used to validate the hub genes. Moreover, the mRNA ex-

* Corresponding author. Email: yymucun@ymun.edu.cn

pression and the protein expression associated with the hub genes were verified by RT-PCR assays and immunohistochemistry. Finally, GSEA was conducted to determine differential immune cell infiltration and the immunological cells' relationships with hub genes. As the flowchart shows in Figure 1, the purpose of this study was to identify the effective diagnostic biomarkers and immune infiltration in DFU and to provide therapeutic targets for DFU.

Materials and Methods

Microarray data collection

Microarray gene expression data were downloaded from the Gene Expression Omnibus (GEO, <http://www.ncbi.nlm.nih.gov/geo/>) database. The circRNA expression data was obtained from the gene expression dataset GSE114248 which included five DFU tissues and five non-DFU tissues. Similarly, the mRNA data was obtained from the gene dataset GSE80178 which included nine DFU samples and three non-DFU samples. GSE199939 was used as an external validation dataset, including 11 non-DFU samples and 10 DFU samples.

DECs identification

The limma package, a core component of Bioconductor in R software was used to identify the DEGs between non-DFU samples and DFU samples. The DEGs were selected using $|\log_2$ fold change (FC)| of >2 and a P -value of < 0.05 . Then, it was followed by a visualization of the heatmap and volcano plot.

Random forest

A Random Forest is a collection of classification trees generated by bootstrap sampling from data and randomly sampling predictor variables at each node. They can handle large numbers of genes without formal variable selection, they are robust to outliers, do not require data to follow the normal (or any other) distribution, can be used for badly unbalanced data sets, and can impute missing values intelligently. In this study, we used a random forest feature selection algorithm to screen the characteristic genes in DFU. Then, we selected the top 100 of the DFU hub genes intersected with the predicted genes.

Gene ontology enrichment and KEGG analysis

Gene ontology (GO) analysis was used to provide gene annotation terms (8), while the Kyoto Encyclopedia of Genes and Genomes (KEGG) was used for pathway enrichment analysis (9). The clusterProfiler is an ontology-based R software package for statistical analysis and visualization of functional clusters of gene clusters or genomes (10). In this study, the GO analysis and pathway enrichment analysis of mRNA was performed using the clusterProfiler package. The molecular function of predicted mRNAs was evaluated by using GO and KEGG. In addition, a p -value of <0.05 and a q -value of <0.05 were considered to be significant differences.

CircRNA-miRNA-mRNA regulatory network construction

CircInteractome (<http://circinteractome.nia.nih.gov>) is a commonly used database for querying the relationship between circRNAs and miRNAs, covering a complete GENCODE annotated transcriptome, including more than

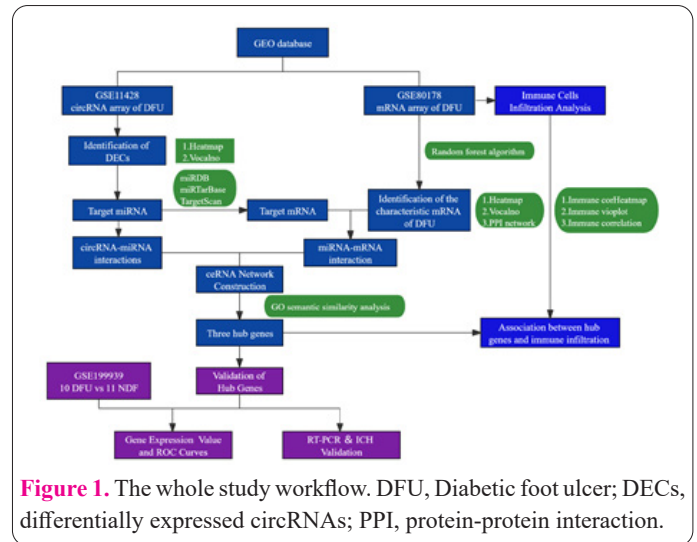


Figure 1. The whole study workflow. DFU, Diabetic foot ulcer; DECs, differentially expressed circRNAs; PPI, protein-protein interaction.

10,000 non-coding RNA genes. In this study, the CircInteractome database was used to identify the probable circRNA-miRNA interaction pairs. In addition, the interaction between miRNA and mRNA was predicted by combining the three databases of miRDB (<http://mirdb.org/>), miRTarBase (<http://mirtarbase.mbc.nctu.edu.tw/index.html>), and TargetScan (http://www.targetscan.org/vert_72/). Selected target mRNA was also identified for further analysis. Then, the circRNA-miRNA-mRNA network was established by combining the circRNA-miRNA interaction and the mRNA-miRNA interaction. The visualization of the regulatory network was performed using an open-source platform Cytoscape (<https://cytoscape.org>).

GO semantic similarity analysis and identification of hub genes

In this study, we used the semantic similarity based on GO and ranked proteins according to the functional similarity of PPI. The GO semantic similarity was verified by the correlation with gene expression profile, which provided a basis for functional comparison of gene products. Herein, the GOSemSim software package was used to identify hub genes (11). Moreover, we verified the expression of the crucial genes and evaluated the accuracy of crucial genes using receiver operating characteristic (ROC) curves in external dataset GSE199939.

Quantification of the expression of key genes

RT-PCR experiment was used to validate the hub genes from the in-silico analysis. Firstly, wound tissues from 8 DFU patients and 8 normal controls were collected to extract total RNA using TRIzol reagent (Invitrogen, Carlsbad, CA, USA), then reverse-transcribed into cDNA by MonScript™ RTIII Super Mix with dsDNase. Next, qPCR was performed in a Roche LightCycler96 System by MonAmp™ SYBR® Green qPCR Mix (none ROX). The primers were synthesized by Wuhan GeneCreate Biological Engineering Co. Ltd with the sequences listed in Table 1. The expression of mRNA (relative to GAPDH) was analyzed by the method of $2^{-\Delta\Delta Ct}$.

Sample collection and classification

Full-thickness skin tissues were obtained from patients receiving standard care at the Affiliated Hospital of Youjiang Medical University for Nationalities. The protocols were approved by the Medical Ethics Committee of You-

Table 1. The primers used in this study.

Symbol	Primer	Primer sequence (5'-3')
ENPP5	Forward primer	5'-CACTAACTCACGCTCATCC-3'
	Reverse primer	5'-TTGCCTAACAGAAAGTCATC-3'
KIAA1109	Forward primer	5'-ACAATAACCAAGATAACAAGG-3'
	Reverse primer	5'-CATCAACATTACGAAGCAG-3'
NRP1	Forward primer	5'-CCAAACCACTGATAACTCG-3'
	Reverse primer	5'-ACCATACCCAACATTCCA-3'
GAPDH	Forward primer	5'-CAGGAGGCATTGCTGATGAT-3'
	Reverse primer	5'-GAAGGCTGGGGCTCATTT-3'

jiang Medical University for Nationalities (batch number: 2018051501). And every patient signed the informed consent for the acquisition and use of discarded tissue. Our study includes NDF patients (n=8) who underwent foot surgery for acute lower extremity trauma and DFU patients (n=8) who had surgical resection of the ulcer. Patients with any conditions, such as serious infection, or medications that could affect wound healing were excluded from the study. Discarded skin samples from peri-wound tissue were collected following RT-PCR validation.

DFU mouse model

We established the mouse model of DFU according to the previous study of Li (12). Purchased male C57BL/6 mice (Changsha Tianqin Biotechnology Co. Ltd, Changsha, China) at 5 weeks of age and 16-18 g weight were treated with 0.45% streptozotocin (Sigma, St. Louis, MO, USA, 45 mg/kg) and feed with a high-fat diet. We chose these mice with a blood glucose level of 16.7 mmol/L to establish the DFU model. The control group was not treated. Then, we used the sterile punch to make wounds. Wound tissues were collected 10 days after wounding (batch number: 2018051501). The collected specimens were fixed in 4% polyoxymethylene for 24 h and then embedded in paraffin. Histological examination was performed on 4-mm-thick serial sections.

Immunohistochemistry

Sections were deparaffinated, blocked, and incubated with the primary anti-KIAA1109 antibody (Novus, NBP1-82145), anti-ENPP5 antibody (Abcam, Cambridge, MA, USA, ab137014) and anti-NRP1 (Beyotime, Shanghai, China, AF1843) at 4°C overnight. Image J software was utilized to measure the total tissue area and integrated optic density (IOD) of the target gene, which was stained yellow-brown. The intensity of gene expression was presented as IOD per unit area.

GSEA analysis of immune cell infiltration

The GSEA algorithm is commonly used to quantify the pathway enrichment score, which is determined according to the background gene set (13). The score represents the absolute enrichment degree of each gene set in a given data set. The GSEA algorithm analyzed the RNA-seq data of patients in different subgroups to infer the relative proportion of immune infiltrating cells. Correlation analysis explored the relationship between hub genes and immune infiltrating cells and analyzed the immune regulatory mechanism that hub genes may have been involved in. The *P*-value of <0.05 was considered to have a statistical difference.

Statistical analysis

R version 4.0 was used to perform bioinformatics analyses and a *P*-value or adjusted *P*-value < 0.05 was considered statistically significant. Statistic Package for Social Science (SPSS) version 26 (IBM, Armonk, NY, USA) and GraphPad Prism 8.0 (La Jolla, CA, USA) software were used to analyze clinical and experimental data. Unpaired Student's *t*-test was used to compare the two sets of data. *P* < 0.05 was considered statistically significant.

Results

DECs between the normal group and DFU group

A total of 879 DECs including 385 upregulated circRNAs and 494 downregulated circRNAs were identified between the normal group and DFU group. The volcano plot showed significant differences in distribution between each dataset (Figure 2a), which was confirmed by the heatmap (Figure 2b).

Construction of the circRNA-miRNA and miRNA-mRNA networks for DFU

We used the CircInteractome online database to predict miRNA targets of statistically different circRNA (Top five circRNAs of each upregulated and downregulated circRNAs). The results showed that there were 239 miRNA-related targets of circRNA with a total of 572 circRNA-miRNA relationship pairs. Through the visualization of the PPI

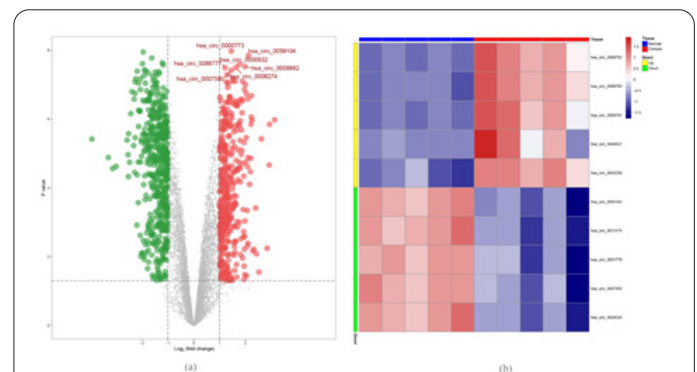
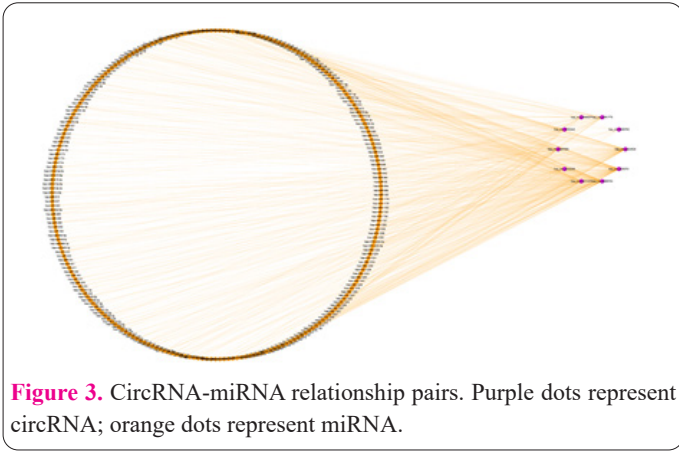


Figure 2. The volcano plot and heatmap for differentially expressed circular RNAs (DECs) between diabetic foot ulcers (DFU) sample and normal sample. (a) The volcano plot of DECs detected in DFU (*P*-value < 0.05 and |LogFC| > 1). The X-axis represents the value of log₂ fold change, while the Y-axis represents the value of -log₁₀. The upregulated genes were marked in red, while the downregulated genes were marked in green. The gray dots represented genes with no significant difference. LogFC, Log₂ (fold change). (b) The heatmap of DECs. Color from blue to red indicated low to high representation value.



network generated by the Cytoscape software, we analyzed the circRNA and miRNA competitive endogenous network and successfully constructed the ceRNA competitive endogenous network diagram (Figure 3). We further used TargetScan, miRDB, and miRTarBase databases to predict miRNA-targeted mRNA. A total of 1440 mRNAs and 1872 miRNA-mRNA linking pairs were screened.

Identification of hub genes

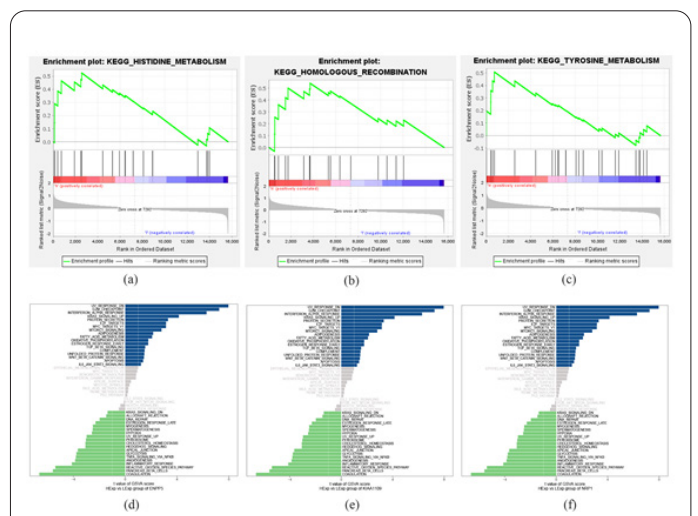
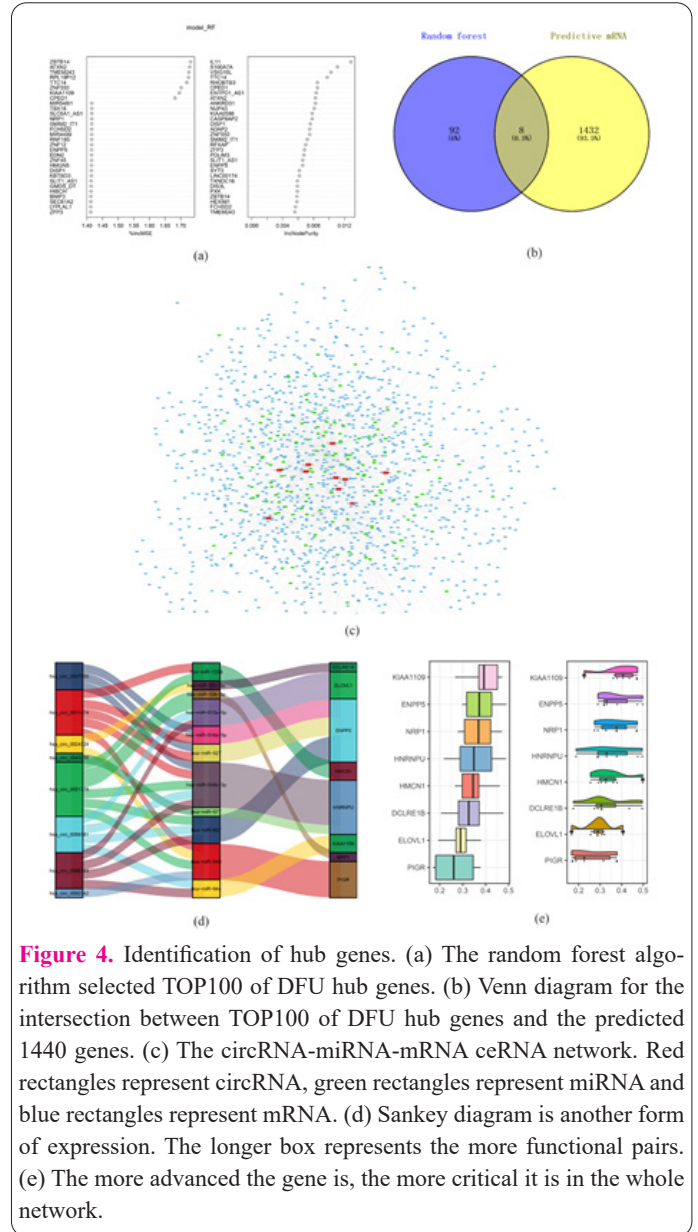
To identify the hub genes, we downloaded the GSE80178 data set from the GEO database, and we used a random forest feature selection algorithm to screen the characteristic genes in DFU. The random forest algorithm selected the top 100 of the DFU hub genes intersected with the predicted 1440 genes. A total of 8 hub genes were screened, including *KIAA1109*, *NRP1*, *ENPP5*, *DCLRE1B*, *HMCN1*, *ELOVL1*, *PIGR*, and *HNRNPU* (Figure 4a, b). Through the PPI visual network generated by Cytoscape software, we analyzed the circRNA-miRNA-mRNA competitive endogenous network and successfully constructed the ceRNA network diagram and the Sankey diagram (Figure 4c, d). Then, the hub genes were screened using GO semantic similarity, and *KIAA1109*, *ENPP5*, and *NRP1* genes were found more critical in the whole network (Figure 4e).

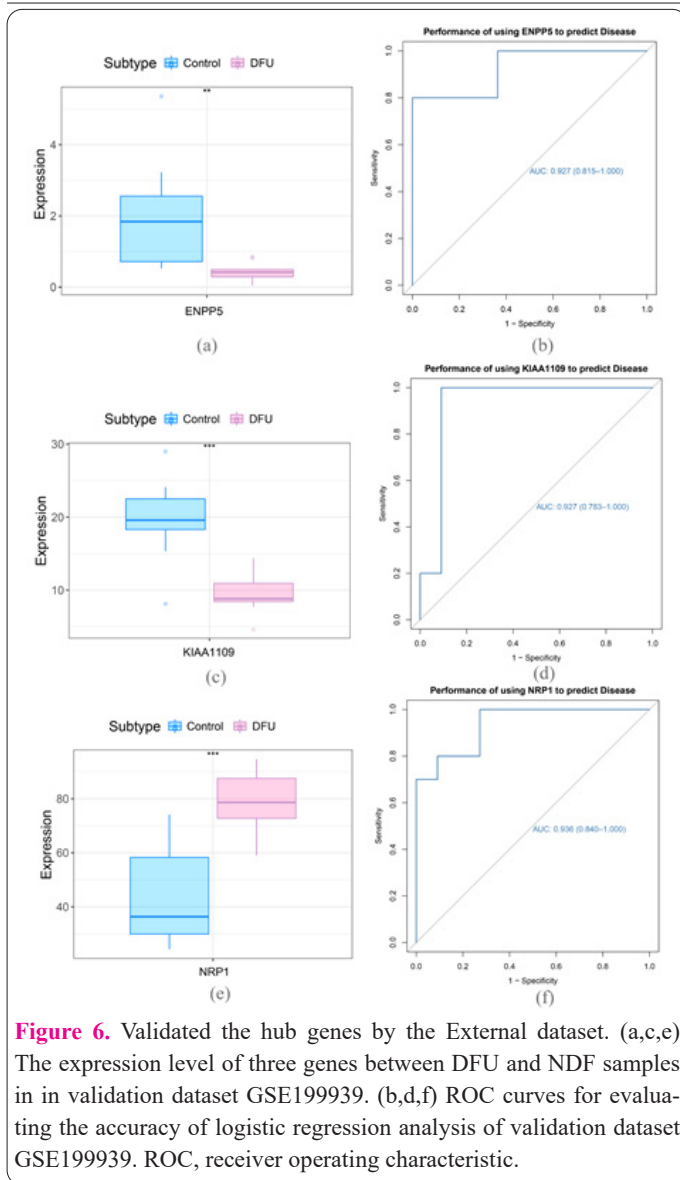
Pathway enrichment analysis of hub genes

We elucidated specific signal enrichment pathways of the three hub genes to explore the potential molecular mechanism regarding the progression of DFU. Then, we found significant enrichment in many related pathways through GSEA. The high-expression *ENPP5*-enriched pathway was the tyrosine metabolism signaling pathway. High expression *KIAA1109*-enriched pathway was a homologous recombination signaling pathway. And high expression *NRP1*-enriched pathway was the histidine metabolism signaling pathway (Figure 5a,b,c).

External dataset validation of key genes

We validated the expression of the key genes and performed ROC analysis on external dataset GSE199939. Results revealed that *ENPP5* and *KIAA1109* were significantly down-regulated in DFU while *NRP1* was significantly upregulated in DFU (Figure 6a,c,e). The ROC curves revealed the probability of *KIAA1109*, *ENPP5* and *NRP1* as valuable biological markers with AUCs of 0.927, 0.927 and 0.936 (Figure 6b,d,f).





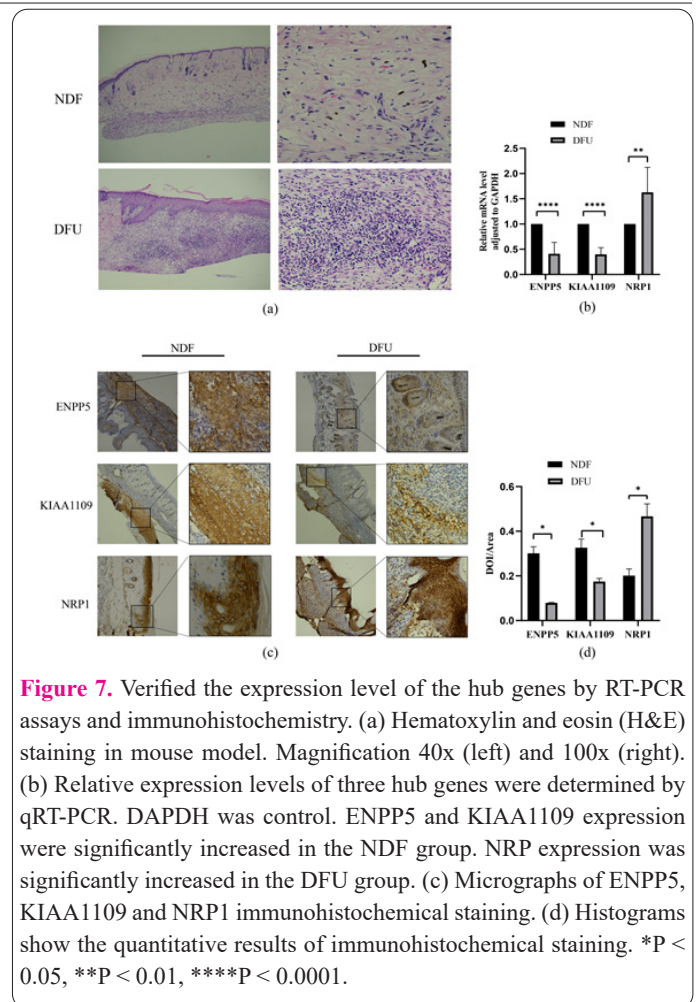
The expression of key genes

Patients' clinical characteristics including age, gender and body mass index (BMI) were retrospectively collected and compared between groups. None of the clinical characteristics differed significantly between the two groups. For the purpose of confirming the hub genes analyzed by bioinformatics tools, we extracted the total RNA of the three genes in DFU samples and healthy tissues to perform RT-PCR analysis. The results indicated that *KIAA1109* and *ENPP5* were significantly down-regulated in DFU and *NRPI* was significantly upregulated in DFU than in healthy controls, which was in accordance with our expectations (Figure 7b).

H&E revealed the accumulation of Neutrophils was more than that of the control group (Figure 7a). Immunohistochemistry was used to assess *KIAA1109*, *ENPP5* and *NRPI* expression. *KIAA1109* and *ENPP5* expression was higher in NDF samples, while *NRPI* expression was higher in DFU (Figure 7c). Quantitative analysis by Image J software showed that the mean DOI of the tissue area (DOI/Area) of DFU samples *NRPI* was significantly higher than that of NDF samples (Figure 7d).

Different immune cell infiltration between DFU and normal groups

In this study, we used GSEA software to reveal the pattern of immune cell infiltration in DFU. After data proces-



sing and screening, 3 cases of NDF data and 9 cases of DFU data were included in the subsequent analysis, and a heatmap was used to show the proportion of 27 immune cells in these two groups of samples (Figure 8a). The proportion of Neutrophils was higher in the DFU group (Figure 8b). Furthermore, we performed a correlation analysis of infiltrated immune cells in DFU, with scores representing the degree of correlation (Figure 8c). The correlation heatmap indicated that activated Tfh cells and CD8+ T cells showed the most synergistic effect, while T cell co-inhibition and Th2 cells showed the most competitive effect.

Correlation between hub genes and immune cells

As indicated from the correlation analysis, *ENPP5* was positively correlated with neutrophils, Th2 cells, and immature dendritic cells (iDCs), and negatively correlated with plasmacytoid dendritic cells (pDCs), follicular helper T cells (Tfh), and mast cells (Figure 9a). *KIAA1109* was positively correlated with Th2 cells, neutrophils, and Treg, and negatively correlated with B cells, CD8+ T cells, and pDCs (Figure 9b). *NRPI* was positively correlated with neutrophils, Treg, and Th2 cells, and negatively correlated with Tfh, CD8+ T cells, and B cells (Figure 9c).

Discussion

DFU biomarkers can be helpful for further understanding of DFU, improving early clinical diagnosis, disease prevention, disease progression prediction and even treatment evaluation of DFU. Therefore, identifying the potential biomarkers associated with DFU development is an

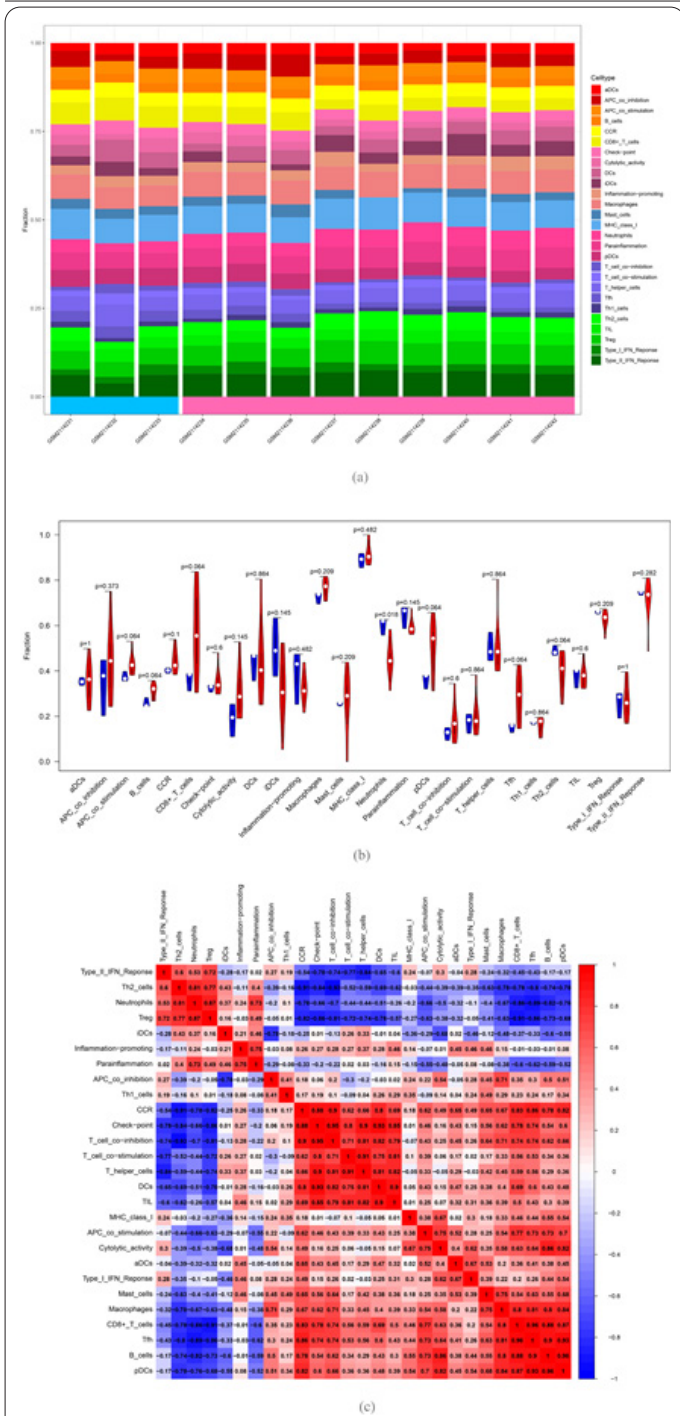


Figure 8. Immune cell infiltration patterns in DFU samples and NDF samples. (a) Histogram of the proportions of 27 immune cell subpopulations in each DFU and NDF sample. x-axis: GEO samples; y-axis: percentage of each immune cell type. (b) Violin plot showing the differentially infiltrated immune cells between the two groups. Blue represents the NDF group and red represents the DFU group. P value < 0.05 was considered as statistically significant. (c) Correlation heatmap of all immune cells. Numbers in the small square represent Pearson's correlation coefficient between the two immune cells on the horizontal and vertical coordinates; red squares indicate a positive correlation and blue squares indicate a negative correlation.

effective method for preventing and treating DFU. In the present study, we identified 879 DEcircRNAs between DFU and normal samples and predicted 1440 mRNAs by CircRNA-miRNA-mRNA ceRNA regulatory. Furthermore, we performed numerous bioinformatics analyses to identify the key genes of DFU and verified by RT-PCR assays and immunohistochemistry. The results indicated that *ENPP5*, *KIAA1109*, and *NRP1* were found to be the

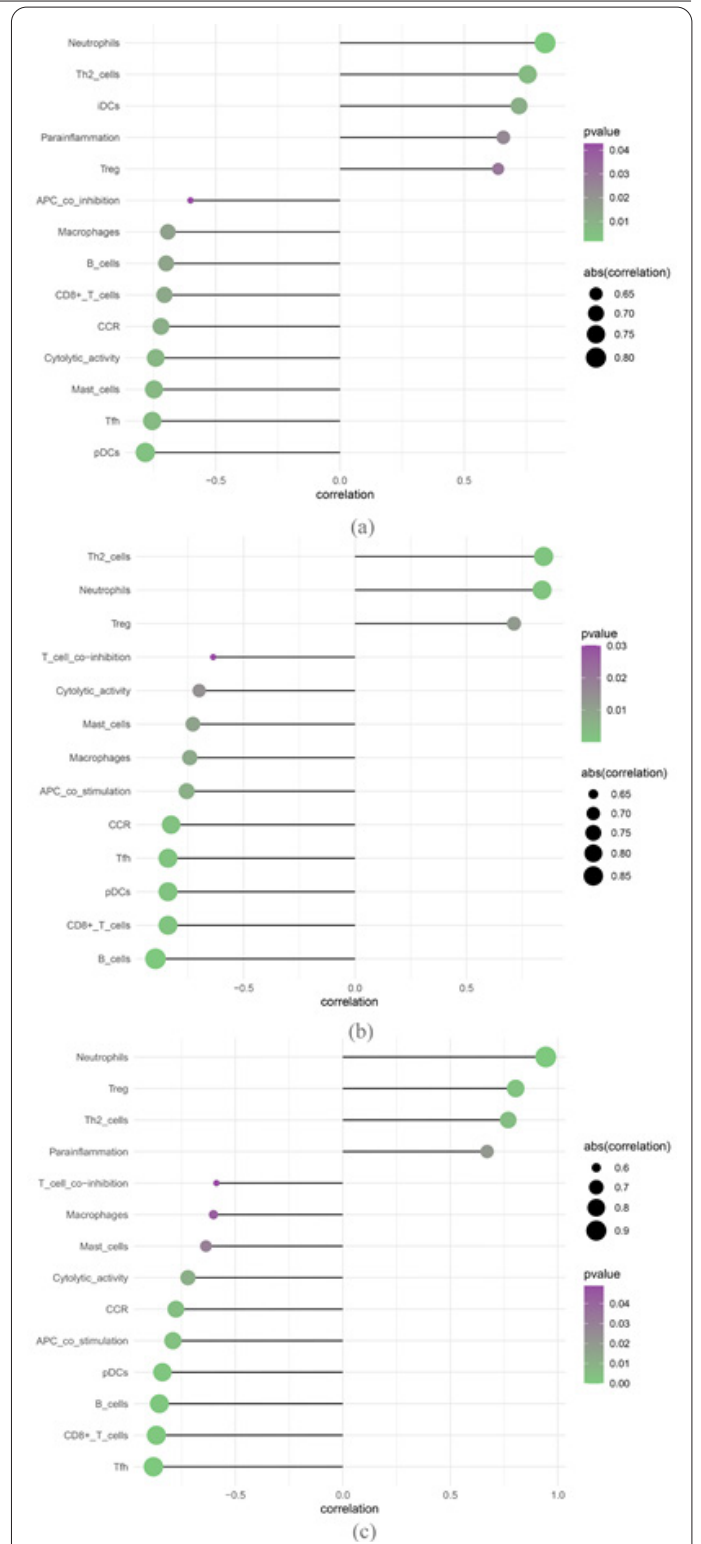


Figure 9. The correlation between the hub genes and infiltrating immune cells. The size of the dots represents the strength of the correlation between genes and immune cells, and the color of the dots represents the P-value. P < 0.05 was considered statistically significant.

key differentially expressed genes. These key genes might have acted as the essential molecules that have mediated the progression of DFU. In addition, we revealed for the first time the correlations between the hub gene and immune cells in DFU by immune cell infiltration analysis. These results provided a new comprehensive perspective for understanding the pathogenesis of DFU and provided valuable clues for finding potential biomarkers and therapeutic targets for DFU.

Extracellular nucleotide pyrophosphatase/phosphodiesterase family (E-NPPs) is widely involved in many

regulatory processes, such as nucleotide cycle, pyrophosphate level regulation, phospholipid signaling regulation, cell movement stimulation, insulin receptor regulation, and activation of some extracellular kinases. Abnormal expression of E-NPPs was found in many diseases, such as bone mineralization disorder, abnormal cell movement and metastasis, angiogenesis, tumor invasion, type 2 diabetes, and others (14-16). A previous study found that *NPPI* had the effect of anti-insulin and inhibited the phosphorylation of insulin receptors stimulated by insulin (17). It was also found that carriers of the Q variant of *ENPP1* had an increased risk of developing end-stage kidney disease early in the course of type 1 diabetes (18). The *ENPP5* is a member of this family and is widely expressed in a variety of organs (19). However, there are only a few studies regarding the biological activity of *ENPP5* and its role in the physiological and pathological processes. The effect of *ENPP5* on DFU was worthy of our exploration. *KIAA1109* is encoded on the chromosomal region 4q27. This region and the *KIAA1109*-interleukin 2 (IL2)-IL21 block, in particular, were identified as a possible locus of risk for the development of a number of common inflammatory disorders, such as type I diabetes, ulcerative colitis, systemic lupus erythematosus, celiac disease, Crohn's disease, psoriasis, and rheumatoid arthritis (20-25). Previous studies found that the mutation of *KIAA1109* was related to the survival rate of patients with endometrial carcinoma, esophageal squamous cell carcinoma, and prostate cancer (26-28). The neuropilin (*Nrp*) family serves as essential cell surface receptors, which have multifunction in human health and play crucial roles in many key biological processes, including cardiovascular function, neuronal physiology, and immune system function (29). Previous reports showed that *Nrp1* was closely related to metabolic diseases such as diabetes. The decrease of *Nrp1* expression is a characteristic of diabetic nephropathy. Reversal or prevention of podocyte injury is related to the recovery of *Nrp1* expression (30). Injected soluble *Nrp1* reduced retinal vascular leakage in diabetic animals by isolating *VEGFA* from *ANGPTL4* or *SEMA3A* (31,32). In addition, *Nrp1* is expressed in a variety of immune cells, in which it regulates a variety of functions, including development, migration and recruitment, communication between different immune cells, and regulation of immune response (33). There is evidence that *Nrp1* of macrophages inhibits insulin tolerance induced by a high-fat diet by inhibiting the preexcitation and activation of *Nrp3* inflammatory bodies, which indicates that *Nrp1* may be a potential target for the treatment of metabolic diseases such as diabetes (34). These results provided evidence that these three hub genes played crucial roles in the diagnosis and prognosis of DFU.

To investigate the potential causative roles of hub genes, the dysregulated biological pathways were identified by enrichment analysis. Our results showed that these hub genes were enriched in multiple signaling pathways, such as tyrosine metabolism, homologous recombination, and histidine metabolism signaling pathways. Studies found that Bruton's tyrosine kinase inhibitor, ibrutinib, upregulated the expression of VEGF and inhibited the expression of TLRs by regulating the RAGE/NF- κ B pathway, thereby inhibiting the secretion of inflammatory factors IL-1 β , TNF- α , and IL-6, and promoting the healing of diabetic foot (35). Tyrosinase and tyrosinase-

related protein 1 were considered as central genes and enriched in tyrosine metabolism that was involved with skin acute wound healing (36). Further, several recent studies revealed that the development of DM was closely related to amino acid metabolism (37). The histidine metabolic pathway contributes to the process of diabetic retinopathy (38). Homologous recombination (HR) is the main way to repair DNA double-strand breaks in mammalian cells. Many HR gene mutations are associated with tumor susceptibility. Congenital defects are associated with HR damage (39). According to research studies, homologous recombination maintained genomic stability and inhibited tumorigenesis. It is very important to fully understand the human disease-related components and HR mechanisms, including functions associated with the HR pathway (40). Consistent with these findings, our results confirmed that these pathways were important molecular regulatory mechanisms in patients with DFU, and their specific effects on DFU were worthy of this elucidation.

The DFU microenvironment is mainly composed of fibroblasts, immune cells, extracellular matrix, a variety of growth factors, and inflammatory factors, and has special physical and chemical characteristics. The nature of the microenvironment significantly affects the diagnosis, survival outcome, and treatment efficacy of the disease. It was reported that an excessive number of neutrophils was released and extracellularly trapped in diabetic wounds, which activated NLRP 3 inflammasome in macrophages and released IL-1 β , which may have prolonged the inflammatory period and inhibited the granulation tissue formation (41). In our study, we performed a comprehensive analysis of immune cell infiltration. In this analysis, Macrophages, neutrophils, Treg, CD8+ T cells, and MHC class I represented the top five highest infiltrating fractions in DFU and neutrophils infiltration in the DFU group was significantly higher than in the normal group. In addition, the three hub genes had their own unique characteristics of immune cell infiltration. *ENPP5* was positively correlated with neutrophils, Th2 cells, and iDCs, while negatively correlated with pDCs, Tfh, and mast cells. *KIAA1109* was positively correlated with Th2 cells, neutrophils, and Treg, while negatively correlated with B cells, CD8+ T cells, and pDCs. *NRPI* was positively correlated with neutrophils, Treg, and Th2 cells, while negatively correlated with Tfh, CD8+ T cells, and B cells. This result reveals that wound cell abnormalities in DFU and immune cells, especially neutrophils, play a critical role in wound healing. However, the role of the relationship between hub genes and immune infiltration in the occurrence and development of DFU needs to be further elucidated. Although more studies are needed to determine the phenotypic abnormalities of cells in the diabetic wound, these findings have clear implications for therapeutic intervention.

In summary, we identified three hub genes, including *ENPP5*, *KIAA1109*, and *NRPI*. The biological functions and pathways of the identified genes provided a more detailed molecular mechanism for understanding the development of DFU. Further, we found a difference in the immune infiltration process between the DFU and normal control groups, and the hub genes were closely related to immune infiltration. Importantly, we validated the key genes experimentally, confirming that the proteins encoded by these genes are different expressed in DFU tissue. Therefore, the three hub genes might be potential key bio-

markers in the development of DFU, and our study would provide a novel perspective on the pathogenesis and therapeutic strategies of DFU.

Data availability statement

Publicly available datasets were analyzed in this study. These data can be found in the GEO database (<https://www.ncbi.nlm.nih.gov/geo/>).

Authors' contributions

XL and BW contributed to the conception and design of the study. XL and BC acquired the data. XL, YX, and AZ analyzed the data. XL and BC interpreted the results. XL and BW wrote the manuscript with all authors providing feedback for revision. All authors read and approved the final manuscript.

Funding

This study was supported by the National Natural Science Foundation of China (NSFC81960875).

Acknowledgments

We sincerely thank the scientists who shared their data on the public database.

References

- Ishaq R, Haider S, Saleem F, et al. Diabetes-related Knowledge, Medication Adherence, and Health-related Quality of Life: A Correlation Analysis. *Altern Ther Health M* 2021; 27(46-53).
- Prevost J, Lambert J. TENS and EMS Treatment for Diabetic Peripheral Neuropathy. *Altern Ther Health M* 2022; 28(6): 57-59.
- Han D, Li J, Wang H, et al. Circular RNA circMTO1 acts as the sponge of microRNA-9 to suppress hepatocellular carcinoma progression. *Hepatology* 2017; 66(4): 1151-1164.
- Chen X, Huang J, Peng Y, Han Y, Wang X, Tu C. The role of circRNA polyribonucleotide nucleoside transferase 1 on gestational diabetes mellitus. *Cell Mol Biol* 2022; 68(6): 148-154.
- Liao S, Lin X, Mo C. Integrated analysis of circRNA-miRNA-mRNA regulatory network identifies potential diagnostic biomarkers in diabetic foot ulcer. *Non-Coding Rna Res* 2020; 5(3): 116-124.
- Li L, Xie Z, Qian X, et al. Identification of a Potentially Functional circRNA-miRNA-mRNA Regulatory Network in Melanocytes for Investigating Pathogenesis of Vitiligo. *Front Genet* 2021; 12: 663091.
- Xiong DD, Dang YW, Lin P, et al. A circRNA-miRNA-mRNA network identification for exploring underlying pathogenesis and therapy strategy of hepatocellular carcinoma. *J Transl Med* 2018; 16(1): 220.
- Ashburner M, Ball CA, Blake JA, et al. Gene ontology: tool for the unification of biology. The Gene Ontology Consortium. *Nat Genet* 2000; 25(1): 25-29.
- Kanehisa M, Goto S. KEGG: kyoto encyclopedia of genes and genomes. *Nucleic Acids Res* 2000; 28(1): 27-30.
- Yu G, Wang LG, Han Y, He QY. clusterProfiler: an R package for comparing biological themes among gene clusters. *Omics* 2012; 16(5): 284-287.
- Yu G, Li F, Qin Y, Bo X, Wu Y, Wang S. GOSemSim: an R package for measuring semantic similarity among GO terms and gene products. *Bioinformatics* 2010; 26(7): 976-978.
- Li B, Luan S, Chen J, et al. The MSC-Derived Exosomal lncRNA H19 Promotes Wound Healing in Diabetic Foot Ulcers by Upregulating PTEN via MicroRNA-152-3p. *Mol Ther-Nucl Acids* 2020; 19: 814-826.
- Barbie DA, Tamayo P, Boehm JS, et al. Systematic RNA interference reveals that oncogenic KRAS-driven cancers require TBK1. *Nature* 2009; 462(7269): 108-112.
- Chaney T, Chaney S, Lambert J. The Use of Personalized Functional Medicine in the Management of Type 2 Diabetes: A Single-Center Retrospective Interventional Pre-Post Study. *Altern Ther Health M* 2022; 28(6): 8-13.
- Goding JW, Grobden B, Slegers H. Physiological and pathophysiological functions of the ecto-nucleotide pyrophosphatase/phosphodiesterase family. *Biochim Biophys Acta* 2003; 1638(1): 1-19.
- Kausar MA, Shahid S, Anwar S, et al. Identifying the alpha-glucosidase inhibitory potential of dietary phytochemicals against diabetes mellitus type 2 via molecular interactions and dynamics simulation. *Cell Mol Biol* 2021; 67(5): 16-26.
- Gijsbers R, Ceulemans H, Stalmans W, Bollen M. Structural and catalytic similarities between nucleotide pyrophosphatases/phosphodiesterases and alkaline phosphatases. *J Biol Chem* 2001; 276(2): 1361-1368.
- Canani LH, Ng DP, Smiles A, Rogus JJ, Warram JH, Krolewski AS. Polymorphism in ecto-nucleotide pyrophosphatase/phosphodiesterase 1 gene (ENPP1/PC-1) and early development of advanced diabetic nephropathy in type 1 diabetes. *Diabetes* 2002; 51(4): 1188-1193.
- Ohe Y, Ohnishi H, Okazawa H, et al. Characterization of nucleotide pyrophosphatase-5 as an oligomannosidic glycoprotein in rat brain. *Biochem Bioph Res Co* 2003; 308(4): 719-725.
- Festen EA, Goyette P, Scott R, et al. Genetic variants in the region harbouring IL2/IL21 associated with ulcerative colitis. *Gut* 2009; 58(6): 799-804.
- Hollis-Moffatt JE, Geary RB, Barclay ML, Merriman TR, Roberts RL. Consolidation of evidence for association of the KIAA1109-TENR-IL2-IL21 rs6822844 variant with Crohn's disease. *Am J Gastroenterol* 2010; 105(5): 1204-1205, 1206-1207.
- Liu Y, Helms C, Liao W, et al. A genome-wide association study of psoriasis and psoriatic arthritis identifies new disease loci. *Plos Genet* 2008; 4(3): e1000041.
- Sawalha AH, Kaufman KM, Kelly JA, et al. Genetic association of interleukin-21 polymorphisms with systemic lupus erythematosus. *Ann Rheum Dis* 2008; 67(4): 458-461.
- van Heel DA, Franke L, Hunt KA, et al. A genome-wide association study for celiac disease identifies risk variants in the region harboring IL2 and IL21. *Nat Genet* 2007; 39(7): 827-829.
- Zhernakova A, Alizadeh BZ, Bevova M, et al. Novel association in chromosome 4q27 region with rheumatoid arthritis and confirmation of type 1 diabetes point to a general risk locus for autoimmune diseases. *Am J Hum Genet* 2007; 81(6): 1284-1288.
- Qing T, Zhu S, Suo C, Zhang L, Zheng Y, Shi L. Somatic mutations in ZFX4 gene are associated with poor overall survival of Chinese esophageal squamous cell carcinoma patients. *Sci Rep-Uk* 2017; 7(1): 4951.
- Qiao Z, Jiang Y, Wang L, Wang L, Jiang J, Zhang J. Mutations in KIAA1109, CACNA1C, BSN, AKAP13, CELSR2, and HELZ2 Are Associated With the Prognosis in Endometrial Cancer. *Front Genet* 2019; 10: 909.
- Tindall EA, Hoang HN, Southey MC, et al. The 4q27 locus and prostate cancer risk. *Bmc Cancer* 2010; 10: 69.
- Parker MW, Guo HF, Li X, Linkugel AD, Vander KC. Function of members of the neuropilin family as essential pleiotropic cell surface receptors. *Biochemistry-Us* 2012; 51(47): 9437-9446.
- Loeffler I, Ruster C, Franke S, Liebisch M, Wolf G. Erythropoietin ameliorates podocyte injury in advanced diabetic nephropathy in the db/db mouse. *Am J Physiol-Renal* 2013; 305(6): F911-F918.
- Sodhi A, Ma T, Menon D, et al. Angiotensin-like 4 binds neu-

- ropilins and cooperates with VEGF to induce diabetic macular edema. *J Clin Invest* 2019; 129(11): 4593-4608.
32. Cerani A, Tetreault N, Menard C, et al. Neuron-derived semaphorin 3A is an early inducer of vascular permeability in diabetic retinopathy via neuropilin-1. *Cell Metab* 2013; 18(4): 505-518.
 33. Roy S, Bag AK, Singh RK, Talmadge JE, Batra SK, Datta K. Multifaceted Role of Neuropilins in the Immune System: Potential Targets for Immunotherapy. *Front Immunol* 2017; 8: 1228.
 34. Wilson AM, Shao Z, Grenier V, et al. Neuropilin-1 expression in adipose tissue macrophages protects against obesity and metabolic syndrome. *Sci Immunol* 2018; 3(21):
 35. Yang X, Cao Z, Wu P, Li Z. Effect and Mechanism of the Bruton Tyrosine Kinase (Btk) Inhibitor Ibrutinib on Rat Model of Diabetic Foot Ulcers. *Med Sci Monitor* 2019; 25: 7951-7957.
 36. Zhu HJ, Fan M, Gao W. Identification of potential hub genes associated with skin wound healing based on time course bioinformatic analyses. *Bmc Surg* 2021; 21(1): 303.
 37. Chen T, Ni Y, Ma X, et al. Branched-chain and aromatic amino acid profiles and diabetes risk in Chinese populations. *Sci Rep-Uk* 2016; 6: 20594.
 38. Sun Y, Zou H, Li X, Xu S, Liu C. Plasma Metabolomics Reveals Metabolic Profiling For Diabetic Retinopathy and Disease Progression. *Front Endocrinol* 2021; 12: 757088.
 39. Prakash R, Zhang Y, Feng W, Jasin M. Homologous recombination and human health: the roles of BRCA1, BRCA2, and associated proteins. *Csh Perspect Biol* 2015; 7(4): a16600.
 40. Moynahan ME, Jasin M. Mitotic homologous recombination maintains genomic stability and suppresses tumorigenesis. *Nat Rev Mol Cell Bio* 2010; 11(3): 196-207.
 41. Liu D, Yang P, Gao M, et al. NLRP3 activation induced by neutrophil extracellular traps sustains inflammatory response in the diabetic wound. *Clin Sci* 2019; 133(4): 565-582.